Effect of deuteration on the phase behaviour and structure of lamellar phases of phosphatidylcholines - Deuterated lipids as proxies for the physical properties of native bilayers

Bryant, Gary; Taylor, Matthew; Darwish, Tamim; Krause-Heuerb, Anwen; Kent, Ben; Garvey, Christopher

Bryant, G., Taylor, M., Darwish, T., Krause-Heuerb, A., Kent, B., & Garvey, C. (2019). Effect of deuteration on the phase behaviour and structure of lamellar phases of phosphatidylcholines - Deuterated lipids as proxies for the physical properties of native bilayers. Colloids and Surfaces B: Biointerfaces, 177, 196–203. https://doi.org/10.1016/j.colsurfb.2019.01.040
Document Version: Accepted Manuscript

Published Version: https://doi.org/10.1016/j.colsurfb.2019.01.040

Effect of deuteration on the phase behaviour and structure of lamellar phases of phosphatidylcholines – deuterated lipids as proxies for the physical properties of native bilayers

Gary Bryant[a*], Matthew B. Taylor[a], Tamim A. Darwish[b], Anton M. Krause-Heuer[b], Ben Kent[c] and Christopher J. Garvey[d*]

[a] Centre for Molecular and Nanoscale Physics, School of Science, RMIT University, Melbourne, Australia.
[b] National Deuteration Facility, Australian Nuclear Science and Technology Organisation, Lucas Heights, Australia
[c] Institute for Soft and Functional Materials, Helmholtz-Zentrum Berlin, Berlin, Germany
[d] Neutron Scattering, Australian Nuclear Science and Technology Organisation, Lucas Heights, Australia

a - gary.bryant@rmit.edu.au, *corresponding author
b - tde@ansto.gov.au
c - ben.kent@helmholtz-berlin.de
d - cjg@ansto.gov.au, *corresponding author

Keywords: Phospholipids; SAXS; DSC; Neutron scattering; Deuteration; Lamellar phase

Highlights

- The gel-fluid phase transition temperature is 4.3 ± 0.1 °C lower for lipids with deuterated chains compared to protiated chains.
- Deuterated chains cause a reduction in both the lamellar repeat spacing and bilayer thickness.
- Deuterated headgroups cause an increase in both the lamellar repeat spacing and bilayer thickness.
- Consequences for the interpretation of Neutron Scattering data with deuterated lipids are discussed.

Declarations of interest: none

Contributions

C.J.G. and G.B. planned the project. M.B.T., B.K., C.J.G. and G.B. conducted the experiments and conducted analysis. B.K. conducted the SLD modelling. T.A.D and A.M.K-H. synthesised and characterized the deuterated lipids. All authors were involved in the data analysis and writing of the manuscript.

Statistical Summary

Words: 7405

Figures: 6

Tables: 2

Abstract

Deuteration of phospholipids is a common practice to elucidate membrane structure, dynamics and function, by providing selective visualisation in neutron scattering, nuclear magnetic resonance and vibrational spectroscopy. It is generally assumed that the properties of the deuterated lipids are identical to those of the protiated lipids, and while a number of papers have compared the properties of different forms, to date this has been no systematic study of the effects over a range of conditions. Here we present a study of the effects of deuteration on the organisation and phase behaviour of four common phospholipids (DSPC, DPPC, DMPC, DOPC), observing the effect of chain deuteration and headgroup deuteration on lipid structure and phase behaviour. For saturated lipids in excess water the gel-fluid phase transition temperature is 4.3 ± 0.1 °C lower for lipids with deuterated chains compared to protiated chains, consistent with previous work. Despite this significant change, well away from the transition structural changes as measured by powder small angle X-ray scattering are small and within errors. To investigate this further, measurements were carried out on oriented multilamellar stacks of DOPC in the fluid phase at reduced hydration. Neutrons are used in conjunction with contrast variation to elucidate the role of the deuteration explicitly. It is found that deuterated chains cause a reduction in and lamellar repeat spacing and bilayer thickness, but deuterated headgroups cause an increase. Consequences for the interpretation of Neutron Scattering data with deuterated lipids are discussed.

Introduction

Isotopic labelling offers a non-destructive and non-perturbative means for studying both structure and dynamics. For the particular case most relevant to biological and soft matter, the chemical exchange of the most naturally abundant isotope of hydrogen ^{1}H (99.985 %) for the less common, ^{2}H (deuterium - 0.015 %) enhances experimental access to a large range of length-scales [1] and time scales [1, 2] in bulk samples. While in other aspects of soft matter the uses and limitations of deuterium labelling have been discussed, here we present an exploration of the limitations of deuteration in the context of a particular class of biologically important molecules, the lamellar forming phospholipids. Phospholipids have an important role as a model system in the study of lipid bilayer membranes and their interactions with other bio- and bioactive molecules, and in capturing the physicochemical properties of this important cellular barrier [3, 4]. Examples of these molecules (as used in this study) are shown in Figure S1. Molecular deuteration may act as a contrast to highlight specific molecular and sub-molecular details of bilayer structure [5] and dynamics [6] in even quite complex mixtures [7].

The biologically relevant aspect of these phospholipids is their ability to self-assemble into lamellae or bilayers with hydrocarbon chains on the interior and phosphatidylcholine headgroups on the exterior, in contact with water. These bilayers partition the interior and exterior of cells and organelles, serving as semi-permeable barriers which allow limited permeability for most molecules [8]. For those biomolecules which can solubilise and hence permeate membranes, the packing of the chain groups is a key factor in determining permeability. Under normal biological conditions the chains are in the fluid phase, where the chains are largely free to move and are in a disordered state. Under conditions of temperature or hydration stress, the membranes can undergo a first order phase transition from the fluid phase to the so called gel phase, where the chains are frozen in place at a fixed angle relative to the bilayer, and are no longer free to move[9]. The fluidity of this environment has effects on biological function such as the operation of protein channels. Important issues are the relative mobility and packing of the lipid chains, and the overall structure of the self-assembled system. Different experimental techniques which utilise molecular deuteration of lipid molecules have varying requirements for the degree and site specificity of deuteration, and particular perspectives on the structure and dynamics of bilayers. For example, the use of ^{2}H NMR lineshapes to study motional detail in phospholipid bilayers involves the special sensitivity of the nuclear quadrupolar interactions to very local dynamics[10]. Traditionally, studies tended to use specific sites of deuteration to simplify analysis[11], though

more recent work has also been conducted using per-deuterated lipids[12]. By contrast, vibrational spectroscopy investigations of phase transitions rely on the specific vibrational modes [7, 13] and the small changes in transition energy due the additional atom mass of ^{2}H. In particular, C-H stretching modes reveal aspects of the molecular packing associated with the gel to fluid phase transition. For these measurements the presence of many chemically similar sites along the hydrocarbon chain enhances the signal.

As a structural tool, elastic neutron scattering, and in particular small angle neutron scattering (SANS), neutron reflectivity (NR) and medium angle lamellar diffraction, rely on the difference between the coherent scattering cross sections of certain regions of interest, using deuteration to provide contrast between sample components and elucidate molecular detail not normally resolvable. Generally SANS measurements are made on isotropic samples, while lamellar diffraction measurements are made from oriented lamellar systems on a substrate. In SANS measurements powder averaging of structural detail has benefits in signal to noise where deuteration may also lower the background signal due to the high incoherent cross-section of ^{1}H. Such considerations are of lesser importance for diffraction and NR experiments. Generally the deuteration schemes used for such systems involve the substitution of many hydrogen atoms with deuterium in the regions of molecular interest. This strategy has also been used to modulate the relative intensity of quasielastic neutron scattering signals due to lipid headgroups, and study their dynamics [14].

The early work on neutron scattering using deuteration was reviewed by Jacrot in 1976 [15], and the use for NMR was proposed by Chapman in 1972[16], with initial results presented in 1974 [7, 13, 17, 18]. Synthesis and characterization techniques were reviewed in 1983 by Tulloch [19]. After this, the use of lipid deuteration became a standard technique for understanding membrane structure, kinetics and dynamics, with thousands of papers using these techniques. Deuterated lipids have been used to study the effects of chain length [20] and pressure [21] on bilayer properties and on the thermodynamics of monolayers [22], amongst much else. Deuterated lipids have also been used for understanding how other molecules (e.g., solutes, macromolecules, proteins etc) interact with membranes [23-28].

Most such studies inherently assume that the properties of the deuterated lipids are identical to those of the protiated lipids. While it is known that ^{1}H based hydrocarbons have greater partial molar volumes than their ^{2}H counterparts, a consequence of the greater zero point vibrational energy of the C-^{1}H versus the C-^{2}H bond [29], to date there have been relatively few studies

which directly compare the structure of deuterated and protiated phospholipids. An early DSC study by Petersen et al. [30] compared protiated and chain per-deuterated DPPC and DSPC, and found that the fluid-gel transition temperature was reduced by between 5 and 6 °C for the deuterated forms. This finding was later confirmed for per-deuterated DPPC by Davis [31] using solid state NMR and Katsaris et al. [32] using DSC. Subsequently solid state NMR and DSC were used to map out the phase diagram of mixtures of deuterated DPPC and cholesterol [33]. Morrow and Davis [34] by contrast found using DSC that deuteration of DLPC only resulted in a downward shift of 1 °C in the transition temperature. Deuterated lipids have often been used to understand the fundamental structure of bilayers, using NMR [35] and X-ray and Neutron scattering [36]. An example is the study of Kucerka et al. [36] who simultaneously analysed neutron and X-ray scattering data on protiated and deuterated lipids, combined with sophisticated modelling, to elucidate the detailed structure of DPPC and DOPC bilayers in the fluid phase, and determine the area per lipid with high precision.

Many of these studies do not directly compare protiated and deuterated forms, or do so under a limited range of conditions. For example, most structural studies have been in the fluid phase only. To date there has been no systematic study of the effects of phospholipid deuteration which examines the effects of chain length, saturation, headgroup vs chain deuteration in both the gel and fluid phases.

In this paper we present small and wide angle X-ray Scattering (SAXS and WAXS respectively) and Differential Scanning Calorimetry (DSC) measurements for a range of phosphatidylcholines in excess water. We compare the lamellar repeat spacing, chain packing, and gel-fluid transition temperatures and enthalpies between the deuterated and protiated varieties, and do so for saturated lipids (chain-deuterated) of several different chain lengths in both fluid and gel phases, and an unsaturated lipid in the fluid phase with both chain and headgroup deuteration. For the latter, we also carry out neutron membrane diffraction measurements on stacked bilayers which show small but significant differences between the deuterated and protiated forms.

Methods & Materials

Sample Preparation for SAXS and DSC

The following phospholipids were obtained from Avanti Polar Lipids in powder form and used without further purification: 1,2-distearoyl-*sn*-glycero-3-phosphocholine (DSPC); 1,2-

dipalmitoyl-*sn*-glycero-3-phosphocholine (DPPC); and 1,2-dimyristoyl-d_{54}-*sn*-glycero-3-phosphocholine (DMPC); 1,2-oleoyl-*sn*-glycero-3-phosphocholine (DOPC); along with chain-deuterated equivalents of DSPC, DPPC and DMPC. Chain and headgroup deuterated DOPC were obtained from ANSTO's National Deuteration Facility (see below). Samples were prepared by adding 50% Milli-Q water by mass to the powdered lipid to ensure excess water. A combination of sonication, heating, cooling and gravimetric mixing was used to create homogeneous samples. Samples were transferred from the bulk into quartz X-ray capillaries of diameter 1.5 mm (Hilgenberg, GmbH) and sealed using Selleys 5 minute Araldite epoxy (Selleys PTY LTD, Padstow, Australia).

Stacked Bilayers

DOPC (or the deuterated variants) was dissolved in chloroform and sprayed onto a quartz slide (65 x 25 mm^2). Spraying was performed using an artist's airbrush with low pressure regulated nitrogen, and was carried out over several minutes so the chloroform had time to evaporate, resulting in even coverage on the slide surface. Remaining solvent was removed by desiccating the samples in vacuum for at least 1 hour. Sample hydration was controlled by equilibrating the samples in chambers with saturated NaCl, providing a fixed relative humidity of 75% for at least 8 hours. The stacked bilayers self-assemble as water is absorbed from the gas phase. Different water contrasts were achieved using an appropriate mixture of H_2O and D_2O in equilibration solutions.

Synthesis of head deuterated DPPC and DOPC

1,2-dipalmitoyl-*sn*-glycero-3-phosphate (sodium salt) and 1,2-dioleoyl-*sn*-glycero-3-phosphate (sodium salt) were purchased from Avanti Polar Lipids. $[N(CD_3)_3]$Choline tetraphenylborate was synthesised using the published method of Lin *et al* [37].

1,2-Di-*O*-palmitoyl-*sn*-glycero-3-phospho$[N(CD_3)_3]$choline and 1,2-Di-*O*-oleoyl-*sn*-glycero-3-phospho$[N(CD_3)_3]$choline were synthesised from the sodium salt of the corresponding phosphatidic acid and $[N(CD_3)_3]$choline tetraphenylborate via the published method of Lin *et al* [37]. The product was purified using automated medium pressure chromatography (Grace Reveleris), eluting first with $CHCl_3$:MeOH (80:20), followed by $CHCl_3$:MeOH:H_2O (80:20:2) to elute the product.

Head deuterated DPPC: Data were consistent with that previously reported[37]. ^{1}H NMR ($CDCl_3$, 400 MHz) δ 5.24 (br, 1H), 4.40 (br, 3H), 4.17 (br, 1H), 4.00 (br, 2H), 3.86 (br, 2H), 2.32 (m, 4H), 1.60 (br, 4H), 1.30 (br, 48H); 0.91 ppm (m, 6H). ^{2}H NMR ($CDCl_3$, 60 MHz) δ 3.30 ppm. ^{31}P NMR ($CDCl_3$, 162

MHz) δ -1.56 ppm. ER-MS (+ mode) m/z: predicted $[M+H]^+$ $C_{40}H_{72}D_9NO_8P$ 743.6, found 743.6, >99% deuteration. (Spectra for head deuterated DPPC available in supplementary information, Figures S2-5).

Head deuterated DOPC: ^1H NMR ($CDCl_3$, 400 MHz) δ 5.34 (m, 1H), 5.20 (m, 1H), 4.40 (m, 1H), 4.30 (br, 2H), 4.12 (m, 1H), 3.94 (m, 2H), 3.80 (m, 2H), 2.28 (m, 4H), 2.01 (m, 8H), 1.58 (br, 4H), 1.30 (br, 40H), 0.88 ppm (m, 6H). ^2H NMR ($CDCl_3$, 60 MHz) δ 3.34 ppm. ^{31}P NMR ($CDCl_3$, 162 MHz) δ -0.9 ppm. ^{13}C NMR (^1H, ^2H decoupled) ($CDCl_3$, 101 MHz) δ 173.6 (s), 173.2 (s), 130.0 (s), 129.7 (s), 70.6 (s), 66.2 (s), 63.4 (s), 63.0 (s), 59.2 (s), 53.4 (s), 34.3 (s), 34.1 (s), 31.9 (s), 29.8 (s), 29.6 (s), 29.4-29.0 (m), 27.2 (m), 25.0 (m), 22.7 (s), 14.2 (s) ppm. ER-MS (+ mode) m/z: predicted $[M+H]^+$ $C_{44}H_{75}D_9NO_8P$ 795.7, found 795.8, >99% deuteration. (Spectra for head deuterated DOPC available in supplementary information, Figures S6-9).

Synthesis of chain deuterated DOPC

L-α-Glycerophosphorylcholine cadmium chloride complex was purchased from MP Biomedicals. d_{32}-Oleic acid was synthesised in a multi-step procedure, starting from the hydrothermal H/D exchange of azelaic acid and nonanoic acid [38]. d_{64}-1,2-di-*O*-oleoyl-*sn*-glycero-3-phosphocholine was synthesised from d_{32}-oleic acid and L-α-glycerophosphorylcholine cadmium chloride complex according to the published method of Darwish *et a l*[38]. The product was purified using automated medium pressure chromatography (Grace Reveleris), eluting first with $CHCl_3$:MeOH (80:20), followed by $CHCl_3$:MeOH:H_2O (70:30:5) to elute the product. Data was consistent with that previously reported[38].

Chain deuterated DOPC: ^1H NMR ($CDCl_3$, 400 MHz) δ 5.34 (m, 1H), 5.22 (m, 1H), 4.40 (br, 3H), 4.14 (m, 1H), 3.99 (m, 2H), 3.90 (m, 2H), 3.40 (s, 9H), 2.28 (m, 1.8H). ^2H NMR ($CDCl_3$, 60 MHz) δ 5.35, 1.94, 1.52, 1.20, 0.81 ppm. ^{31}P NMR ($CDCl_3$, 162 MHz) δ -1.5 ppm. ^{13}C NMR (^1H, ^2H decoupled) ($CDCl_3$, 101 MHz) δ 173.6 (s), 173.2 (s), 129.6 (s), 129.5 (s), 70.2 (m), 66.3 (m), 63.8 (m), 62.8 (m), 59.7 (m), 54.5 (s), 33.8 (m), 33.2 (m), 30.6 (s), 28.8-27.7 (m), 26.2 (m), 23.9 (m), 21.4 (s), 13.0 (s) ppm. ER-MS (+ mode) m/z: predicted $[M+H]^+$ $C_{44}H_{19}D_{66}NO_8P$ 853.02, found 853.1, overall 93.9% with isotopic distribution d_{58} 1.7%, d_{59} 6.7%, d_{60} 17.3%, d_{61} 25.05%, d_{62} 21.4%, d_{63} 15.1%, d_{64} 9.0%, d_{65} 3.1%, d_{66} 0.6%. (Spectra of chain-deuterated DOPC available in supplementary information, Figures S10-14).

SAXS/WAXS/DSC

Simultaneous SAXS, WAXS and DSC were conducted on a Bruker MicroCalix small angle x-ray instrument operating on a Cu Kα microfocus source with *in-situ* DSC (Bruker Gmbh, Germany). DSC data were analysed using the in-built Calisto software (Setaram, France). SAXS data was collected on a Pilatus 100k 2D detector with q range of 0.004 to 0.56 $Å^{-1}$, where q is the scattering vector ($q = 4\pi$

$\sin(\theta)/\lambda$, 2θ is the scattering angle and λ is wavelength of the scattered radiation). WAXS data was collected on a Vantec-1 1D detector with q range of 1.2 to 1.9 $Å^{-1}$. SAXS calibration was done using silver behenate and WAXS calibration was done with a combination of silver behenate and 4-bromobenzoic acid. All samples were run through 4 cycles of warming and cooling at 1°C/minute from temperatures approximately 20 °C below to 20 °C above the gel to fluid transition temperature. In the case of DOPC the instrument limited minimum temperature of -30 °C was used. Reproducibility was tested by ensuring that repeated DSC runs were identical. After these temperature cycles, SAXS data was collected at one temperature well below the transition (gel phase) and one temperature well above (fluid phase). Details are shown in Table S1. SAXS data was radially integrated using Fit2D (ESRF) and reflection positions (q_{max} values) found using the Igor Pro (Wavemetrics) multipeak analysis package. Where 3 or 4 reflections were measurable, repeat spacings and uncertainties were determined by linear regression of the fitted q_{max} values. Where only 2 reflections were measurable, the average value was used, with the uncertainty being half the difference between reflections. For WAXS data in the fluid phase there is only 1 reflection, so the uncertainty was defined as the standard deviation of the Gaussian fit.

Neutron membrane diffraction

Neutron membrane diffraction was performed on the V1 membrane diffractometer at Helmholtz-Zentrum Berlin. A quartz slide with a prepared lipid film was mounted vertically in an aluminium humidity chamber together with a saturated NaCl solution prepared with the appropriate H_2O/D_2O ratio. The humidity chamber was sealed at least eight hours prior to measurement to allow for sample equilibration. Temperature was maintained at 25 °C by a circulating water bath directed through copper tubing surrounding the humidity chamber and controlled by a Julabo temperature controller.

Using a monochromatic neutron beam of 4.56 Å, rocking curves of the first five pseudo-Bragg reflections were recorded on a 19×19 cm^2 area detector at a sample-detector position of 1 m. Each rocking curve was recorded by rotating the sample relative to the incident neutron beam through a small angle around the maximum reflection intensity.

Neutron density profiles in real space, showing the scattering density across the bilayer as a function of the distance from the centre of the bilayer, were reconstructed using the Fourier synthesis [39, 40]. The measured intensity of each pseudo-Bragg reflection was corrected for variation of neutron absorption by the sample as a function of the scattering angle, as well as a Lorentz correction. The square root of the corrected intensity is then equivalent to the magnitude of the structure factor at the reflection's positon in q space:

$$f(h) = \sqrt{I(h)A(h)\sin\theta} \quad (1)$$

where f(h) is the structure factor of the h^{th} reflection, I(h) is the measured reflection intensity, A(h) is the absorption correction, and sin(θ) is the Lorentz correction.

The phase of each structure factor – simply positive or negative for a centro-symmetric cell such as a lamellar bilayer, can be determined by variation of the scattering density at a point of symmetry in the unit cell. In this case, we varied the contrast of the water layer – each increase in the D_2O volume fraction of the water layer adds a positive contribution to the SLD of the water layer. The phase of each structure factor will then determine whether the scattering density increases, in the case of a positive structure factor, or decreases, in the case of a negative structure factor. Phasing diagrams (Figure S18) show the variation of the structure factors as a function of D_2O volume fraction, enabling correct phase identification.

The reconstructed scattering length density profile is calculated from a Fourier summation of the structure factors:

$$\rho^*(z) = \rho_0^* - \frac{2}{dk}\sum_{h=1}^{n} f(h)\left(\cos\frac{2\pi hz}{d}\right) \quad (2)$$

where z is the distance from the centre of the bilayer, ρ_0^* is the calculated average SLD of the unit cell from its known constituents, k is a measurement scaling factor, and d is the repeat spacing of the bilayer.

The scaling factor k is determined from multiple measurements of each sample at different H_2O/D_2O ratios. As the contrast of the water layer contrast increases, this change can be seen in regions of the SLD profile containing water, but remains constant in the regions of the unit cell where the water does not penetrate – i.e. the interior of the bilayer. In these regions, the SLD remains constant regardless of the water SLD, allowing for selection of scaling constants k so that these regions of the profiles overlap for all water contrasts. This scaling results in an absolute SLD scale on a dimensionless unit per-lipid basis, as the area per lipid is not measured.

Results

Effect of chain-deuteration - saturated lipids

Figure 1 shows DSC warming traces for DSPC in excess water, and the comparison with DMPC and DPPC is shown in Figure S15. The onset transition temperatures and enthalpies are summarized in Table

1. For all three saturated lipids the transition temperature is shifted lower by 4.3 ± 0.1 °C for the chain-deuterated lipid, and for deuterated DOPC this shift is 3.7 °C. The pre-transition, which is a small reflection to the left of the main reflection, associated with the membrane ripple phase characteristic of long chain saturated lipids [41], also shows a consistent downward shift, relative to the protiated lipids, by 4-6 °C. The fact that the chain deuterated lipids have lower transition temperatures implies that they are slightly more stable in the fluid phase than the gel phase, and is consistent with previous studies [30-32]. Unsurprisingly, as this transition is dominated by the chain interactions, the shift for the headgroup deuterated DOPC is only 0.8 °C. The measured enthalpies are similar for deuterated and protiated species, with no trend being identified.

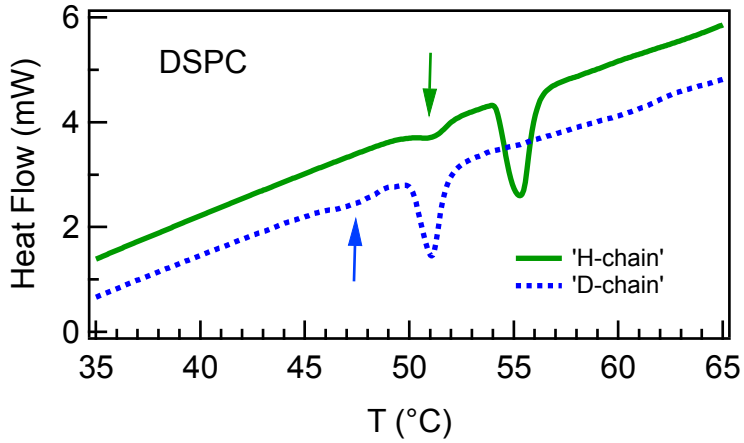

Figure 1: DSC scans during warming for the DSPC (solid green line) and chain-deuterated DSPC (dotted blue line). Arrows indicate the pre-transition.

The measured SAXS intensities as a function of scattering vector q are shown for DSPC in Figure 2 for fluid and gel phases. Insets show the wide angle (WAXS) data. Corresponding graphs for DPPC and DMPC are shown in figures S16. Broadly speaking, the lipids have very similar scattering curves for the protiated and chain-deuterated species, with the observed reflections characteristic of fully hydrated phospholipids. For some samples it can be noted that the reflections are much broader (e.g. DMPC). As these are randomly aligned (powder type) samples rather than aligned samples, the sharpness of the reflections relative to the background is related to the size of the quasi-Bragg reflecting domains within the samples, which is in turn affected by sample history, amount of excess water, distance from phase transitions, etc. In the analysis below we focus on the positions of the Bragg reflections, which are not affected by these factors.

The peak parameters are summarized in Table 2 for the gel and fluid phases respectively. In both the gel and fluid phases, the deuterated lipids have slightly smaller repeat spacings for DMPC and DPPC, and slightly larger for DSPC. These differences are all within the uncertainties except for DSPC in the gel

phase, these differences are outside the errors. This apparent difference in behaviour for the longest chain lipid will be the subject of future work using higher resolution techniques. All samples show two characteristic chain packing reflections in the gel phase, and the positions of the reflections are the same within the errors, although the chain packing reflection 2 shows a slight decrease.

Lipid	Chain length	T_H (°C)	T_D (°C)	T_H-T_D (°C)	H_H (J/g)	H_D (J/g)
DMPC	14	23.7	19.4	4.3	25.9	33.1
Pre-tran		14.3	8.3	6.0	--	--
DPPC	16	41.3	36.9	4.4	45.3	41.0
Pre-tran		35.1	28.9	6.2	--	--
DSPC	18	54.2	50.0	4.2	45.1	43.7
Pre-tran		49.6	45.5	4.1	--	--
DOPC	18	-18.3	--	--	43.2	--
D-chain		--	-22.0	3.7	--	30.6
D-head		--	-19.1	0.8	--	38.1

Table 1 DSC onset transition temperatures and enthalpies for the lipids used in this study.

Figure 3 shows similar data for DOPC in the fluid phase, with the repeat spacings and chain packings shown in Table 2 (note that the gel phase is not considered for DOPC, as the transition fluid-gel temperature is ~ -20°C, and the presence of ice can complicate interpretation). Again the curves are similar, but the differences in the repeat spacings, while still within the uncertainties, are now considerably larger, with deuterated chains reducing the repeat spacing and the deuterated headgroup increasing it. The WAXS data (inset) indicates that there is a shift to lower q for the chain-packing reflection with deuteration, leading to an increase in the chain-chain packing from 4.32 Å to ~4.52 Å, though still within the uncertainties.

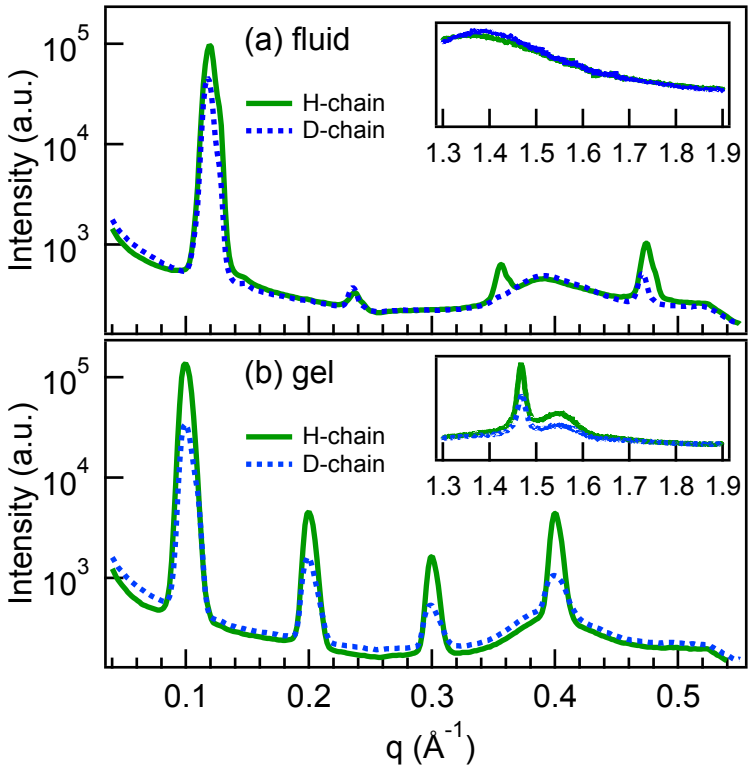

Figure 2 SAXS scattered intensities vs. scattering vector for DSPC in the (a) fluid and (b) gel phase for protiated lipids (solid green lines) and chain-deuterated lipids (dotted blue lines). Insets show the wide angle (WAXS) data. Scan temperatures are in Table S1. The broad reflection at 0.39Å is due to the Kapton windows on the DSC cell. Graphs for DPPC and DMPC are in Figure S16.

Lipid	Gel phase Repeat spacing	Gel phase Chain 1	Gel phase Chain 2	Fluid phase Repeat spacing	Fluid phase Chain packing
DMPC	59.01 ± 0.62	4.16 ± 0.08	4.22 ± 0.02	60.95 ± 0.15	4.5 ± 0.2
D-chain	58.99 ± 0.16	4.13 ± 0.08	4.23 ± 0.02	59.71 ± 0.15	4.5 ± 0.2
DPPC	62.88 ± 0.15	4.14 ± 0.08	4.24 ± 0.02	64.32 ± 0.15	4.6 ± 0.2
D-chain	62.75 ± 0.18	4.12 ± 0.08	4.23 ± 0.02	64.05 ± 0.15	4.6 ± 0.2
DSPC	62.69 ± 0.25	4.04 ± 0.08	4.28 ± 0.02	52.94 ± 0.15	4.6 ± 0.2
D-chain	62.77 ± 0.12	4.05 ± 0.08	4.28 ± 0.02	53.35 ± 0.15	4.5 ± 0.2
DOPC	--	--	--	63.78 ± 0.88	4.32 ± 0.2
D-chain	--	--	--	62.79 ± 0.34	4.47 ± 0.2
D-head	--	--	--	64.23 ± 0.11	4.52 ± 0.2

Table 2 Repeat spacings and chain packing spacings (in Å) as measured by SAXS/WAXS.

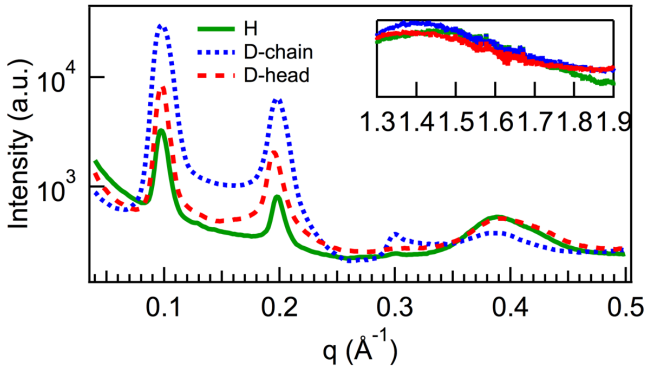

Figure 3 SAXS scattered intensities vs. scattering vector for DOPC (solid green lines), D-chain (dotted blue lines) and D-head (dashed red lines) in the fluid phase. Insets show the wide angle (WAXS) data. Scan temperatures are in Table S1. The broad reflection at 0.39Å is due to the Kapton windows on the DSC cell.

The above experiments were conducted in excess water on "powder" type samples, where local structural variations lead to fairly broad Bragg reflections. It is thus not possible to draw conclusions from these small apparent differences. However, if these differences are real, then it could have implications for interpretation of neutron scattering data. To investigate this, we have conducted neutron membrane diffraction measurements of stacked lipid bilayers at reduced hydration. The reduced hydration increases the order, and the stacked bilayers provide hundreds of layers to Bragg reflect, resulting in sharper reflections [23, 40, 42]. Although neutron scattering provides lower inherent resolution than X-ray scattering, using neutrons allows the contrast to be changed by changing the D_2O/H_2O ratio [43], which allows the correct phasing of the Bragg reflections [44], which provides a unique reconstruction of the scattering length density profiles for each sample.

Three DOPC variants were measured with neutron membrane diffraction –DOPC, head-deuterated DOPC (D-head) and chain-deuterated (D-chain). Each sample was measured at three H_2O/D_2O ratios – 8, 20 and 50% D_2O. The rocking curves of the three samples in 8% D_2O water solution are shown in Figure S17. Four reflections were recorded for DOPC and head deuterated DOPC, and five for chain deuterated DOPC.

The pseudo-Bragg reflections have a Gaussian profile with a FWHM of 0.3 degrees, indicating highly ordered systems irrespective of deuteration, although the positions of the reflections change with deuteration. The repeat spacings and standard errors determined by linear regression are shown Table S3. The uncertainties are much smaller than for the powder samples, and the repeat spacing of each sample is stable between measurements. However, previous work has shown that measurements between equivalent

samples can vary by up to 0.2 Å [43]. In this study, deuteration of the headgroup increases the repeat spacing by 0.33 Angstroms, while deuteration of the lipid chain reduces the repeat spacing by 0.5 Angstroms when compared to the protiated sample. These variations are outside the maximum uncertainty of 0.2 Å, and clearly show that deuteration of DOPC has a small but significant effect on the bilayer repeat spacing.

Fourier reconstructed SLD profiles for the three samples, centred around the middle of the bilayer, are shown in Figure 4. At this D_2O ratio, the water contrast for neutron scattering is nominally zero, and therefore does not contribute to the SLD profile. The large changes in molecular contrast due to deuteration are clearly evident in the profiles. This allows a more precise understanding of how each component of the DOPC molecule contributes to the SLD profile. To examine this effect, we use the approach of Wiener and White [39, 40, 45], who divided the DOPC molecule into quasi-molecular fragments which each contribute a Gaussian distribution to the total SLD profile. The area of each Gaussian profile was fixed at the calculated SLD of the fragment, while the widths and locations of the Gaussians were determined by a fitting procedure. The experiments of Wiener and White were carried out at slightly lower relative humidity (66% RH) and temperature (23 °C), yielding a slightly lower repeat spacing (49.1 Å vs 49.39 Å), however, this proved similar enough to provide satisfactory initial estimates for the location and widths of the Gaussian contributions. The CH_2 groups were modelled using 3 Gaussians to represent the inner, middle and outer regions of the chains. The components are shown in Table S2, and examples of the fitting is shown in Figures S19-S20,

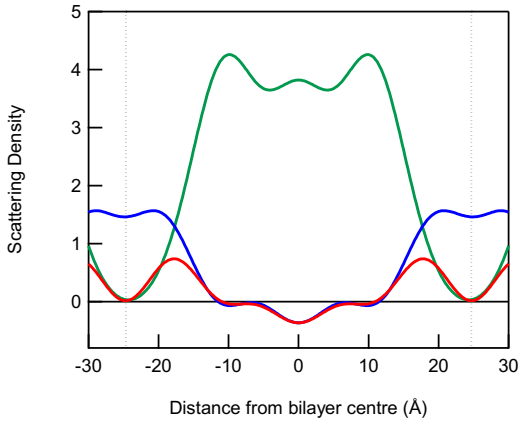

Figure 4. Scattering length density profiles of the three DOPC variants, conducted at 75% RH, with 8% D_2O.

Further refinement of the SLDs for the quasi-molecular fragments was carried out by using the differences between the three profiles to determine the contribution of the fragments to the change

of contrast due to deuteration. First, the chain group SLDs were determined using fits to the difference between the chain deuterated and protiated profiles (Figure S19, left). Second, the SLDs of the headgroup fragments were determined from the difference of the head deuterated profile and the protiated profile (Figure S19, right). These values were then used to fit the components of the protiated DOPC profile that undergo deuteration. The additional constant contrast components (the double bond, glycerol, and phosphate) were then fit using the protiated DOPC SLD profile. The final fit for DOPC is shown in Figure 5.

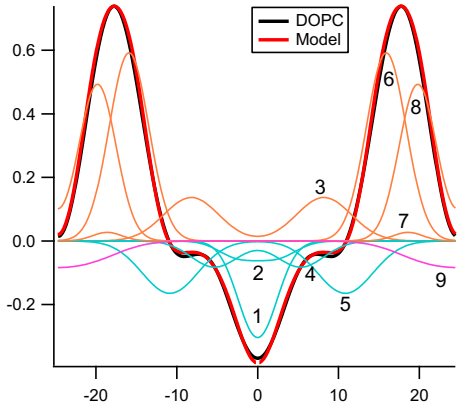

Figure 5. Protiated DOPC SLD profile (solid black line), reconstructed SLD profile (solid red line) and Gaussian contributions of the quasi-molecular fragments (think lines). The fragments are fit using: chain deuterated/DOPC difference (blue lines); head deuterated/DOPC difference (purple line); protiated DOPC (orange lines). The numbers refer to the molecular components, as described in Table S2.

Selective deuteration of a DOPC molecule would be expected to change the SLD of the deuterated quasi-molecular fragments. If a system remained otherwise identical in structure and function, as is often assumed, it should be able to be modelled with changes to the area of each Gaussian contribution which are equivalent to the changes in the SLD of the deuterated components. The widths and locations would remain constant regardless of deuteration level or deuteration location.

However this is not the case - it is found that it is necessary to vary the positions and width of molecular fragments of the bilayer to enable satisfactory fitting of the three bilayer profiles. This is illustrated in Figure 6 for (top) D-chain and (bottom) D-head, where the deuterated models, after adjusting the SLD of the deuterated fragments (yellow filled regions), do not fit the protiated DOPC profile (black lines), and vice versa. In order to obtain a reasonable agreement, the headgroup position in both cases needs to be adjusted. To provide a reasonable fit to the protiated

DOPC, the headgroup components must be shifted: away from the centre of the bilayer for chain deuteration (D-chain - Figure 6 (top, red line); or towards the centre of the bilayer for headgroup deuteration (D-head - Figure 6 (bottom, red line).

Due to the number of Gaussian components, it is difficult to pinpoint the exact effect of deuteration on each component. There is however a clear indication that deuteration results in a structural change of the time average unit cell – effectively thinning the bilayer for tail deuteration, and thickening it for head deuteration, consistent with the data in Table 2 and Table S3.

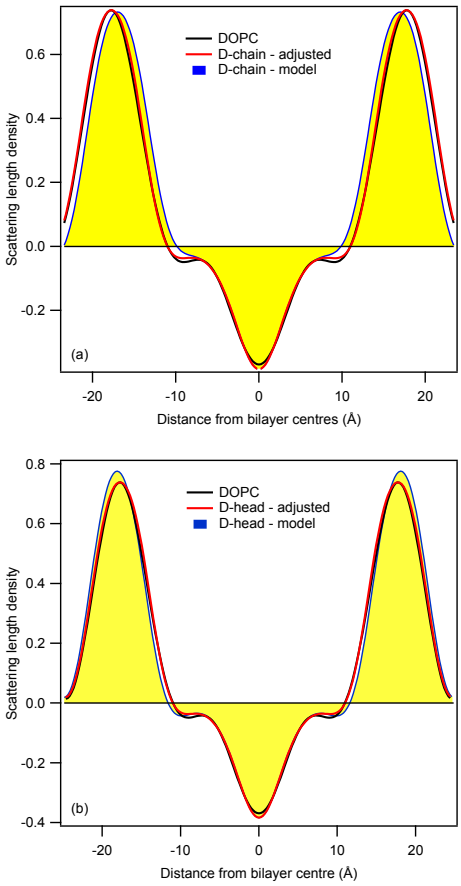

Figure 6. Comparing SLDs for (a) D-chain and (b) D-head with DOPC. DOPC profile (solid black lines); Models, after adjusting the SLD of the deuterated fragments (yellow filled regions); Adjusted (red lines).

Discussion and Conclusions

In this paper we presented a systematic study of the effects of per-deuteration of lipid chains on the structure and phase behaviour of four common lamellar phase forming phospholipids in the fully hydrated state. We also examined the effect of per-deuteration of the headgroup of the fully

hydrated lamellar phases of DOPC. For the saturated lipids it was found that the main gel-fluid phase transition temperature is 4.3 ± 0.1 °C lower for lipids with deuterated chains relative to those with protiated chains. The temperature of the pre-transition (gel to ripple transition) also decreased by between 4 and 6 degrees. Despite this significant change, away from the transition (~20 °C above or below) there is very little change in the structure of either the fluid or gel phases: either in the lamellar spacing as determined by the reflection positions using SAXS; or from the chain packing determined from WAXS measurements. For the unsaturated lipid (DOPC) the transition is lowered by 3.7 °C with deuterated chains. Again however, there was no significant change in the membrane's lamellar spacing observed in the fluid phase, though there was a slight increase in chain packing distance. By contrast to chain deuteration, it was found that headgroup deuteration is accompanied by a significant increase in the chain packing repeat spacing from 4.36 Å to 4.51 Å, along with a slight increase in repeat spacing.

These results show that the self-assembly of chain deuterated lipids is a reasonable analogue of the lipid bilayer under most conditions. However it is important to ensure that the measurement conditions are well away from the gel-ripple or ripple-fluid lamellar phase transitions. If the difference in phase transition temperature is not considered there may be important differences in the packing of lipid molecules and possibly membrane dynamics. The implications for techniques which examine dynamics in membranes are obvious: that results obtained from samples incorporating deuteration may only be generalised when the issue of the temperature gap relative to the phase transition temperature is addressed.

The neutron diffraction experiments showed that the changes in repeat spacing observed for the deuterated molecules are small but significant, and that they have a measurable effect on the bilayer thickness. The effects of deuteration in head-group and hydrocarbon chain regions are antagonistic in terms of their effects on the d-spacing – this may have implications for high resolution structural studies, and suggests that d-spacing alone is not a sufficient criteria to establish the equivalence of chain and headgroup deuterated lipids with the protiated equivalent. For structural studies using the SANS technique, the contrast variation technique may be used to modulate the contribution of specific structural constituents to the signal [46]. Examples of this approach may be found in the use of various types of self-assemblies to mimic the cell membrane environment and the interaction of different molecules with this environment [47-49]. In these analyses, the thickness of the bilayer becomes a critical issue, particularly when it determines which part of, for example, an enzyme is exposed to the solvent. The results shown here suggest that such studies may be better carried out with a selective degree of deuteration, rather than per-

deuteration, to ensure that deuteration perturbs bilayer thickness as little as possible. A second strategy may be to use a small fraction of deuterated lipid to provide a simple means to modulate the contribution of lipids to the to a measured bilayer SLD profile. This strategy, which provides a minimal perturbation to bilayer structure, has been successfully applied to locate a protein in bilayer stacks [50].

Acknowledgements

This research was supported by the Australian Research Council through LP140100993, LP160101496 & LE120100186. The National Deuteration Facility is partly supported by the National Collaborative Research Infrastructure Strategy (NCRIS). We thank Thomas Hauß for providing the macros for SLD modelling.

References

[1] J.S. Higgins, H. Benoit, Polymers and neutron scattering, Clarendon Press, Oxford, 1994.
[2] K. Schmidt-Rohr, H.W. Spiess, Multidimensional Solid-State Nmr and Polymers, Academic Press1994.
[3] S. Garg, F. Castro-Roman, L. Porcar, P. Butler, P.J. Bautista, N. Krzyzanowski, U. Perez-Salas, Cholesterol solubility limit in lipid membranes probed by small angle neutron scattering and MD simulations, Soft Matter, 10 (2014) 9313-9317.
[4] S. Garg, L. Porcar, A.C. Woodka, P.D. Butler, U. Perez-Salas, Noninvasive Neutron Scattering Measurements Reveal Slower Cholesterol Transport in Model Lipid Membranes, Biophysical Journal, 101 (2011) 370-377.
[5] G. Zaccai, G. Buldt, A. Seelig, J. Seelig, NEUTRON-DIFFRACTION STUDIES ON PHOSPHATIDYLCHOLINE MODEL MEMBRANES .2. CHAIN CONFORMATION AND SEGMENTAL DISORDER, Journal of Molecular Biology, 134 (1979) 693-706.
[6] M. Doxastakis, V.G. Sakai, S. Ohtake, J.K. Maranas, J.J. de Pablo, A molecular view of melting in anhydrous phospholipidic membranes, Biophysical Journal, 92 (2007) 147-161.
[7] R. Mendelsohn, J. Maisano, USE OF DEUTERATED PHOSPHOLIPIDS IN RAMAN-SPECTROSCOPIC STUDIES OF MEMBRANE STRUCTURE .1. MULTILAYERS OF DIMYRISTOYL PHOSPHATIDYLCHOLINE (AND ITS-D54 DERIVATIVE) WITH DISTEAROYL PHOSPHATIDYLCHOLINE, Biochimica Et Biophysica Acta, 506 (1978) 192-201.
[8] A. Berk, C.A. Kaiser, H. Lodish, A. Amon, H. Ploegh, A. Bretscher, M. Krieger, K.C. Martin, Molecular Cell Biology, Macmillan Learning2016.
[9] C.J. Garvey, T. Lenne, K.L. Koster, B. Kent, G. Bryant, Phospholipid Membrane Protection by Sugar Molecules during Dehydration-Insights into Molecular Mechanisms Using Scattering Techniques, International Journal of Molecular Sciences, 14 (2013) 8148-8163.
[10] A. Watts, NMR of Lipids, in: G.C.K. Roberts (Ed.) Encyclopedia of Biophysics, Springer Berlin Heidelberg, Berlin, Heidelberg, 2013, pp. 1727-1738.
[11] T. Yasuda, H. Tsuchikawa, M. Murata, N. Matsumori, Deuterium NMR of Raft Model Membranes Reveals Domain-Specific Order Profiles and Compositional Distribution, Biophysical Journal, 108 (2015) 2502-2506.
[12] F. Aussenac, M. Laguerre, J.M. Schmitter, E.J. Dufourc, Detailed structure and dynamics of bicelle phospholipids using selectively deuterated and perdeuterated labels. H-2 NMR and molecular mechanics study, Langmuir, 19 (2003) 10468-10479.
[13] R. Mendelsohn, C.C. Koch, DEUTERATED PHOSPHOLIPIDS AS RAMAN-SPECTROSCOPIC PROBES OF MEMBRANE-STRUCTURE - PHASE-DIAGRAMS FOR THE DIPALMITOYL PHOSPHATIDYLCHOLINE(AND ITS D62 DERIVATIVE)-DIPALMITOYL PHOSPHATIDYLETHANOLAMINE SYSTEM, Biochimica Et Biophysica Acta, 598 (1980) 260-271.
[14] S. Konig, W. Pfeiffer, T. Bayerl, D. Richter, E. Sackmann, MOLECULAR-DYNAMICS OF LIPID BILAYERS STUDIED BY INCOHERENT QUASI-ELASTIC NEUTRON-SCATTERING, J. Phys. II, 2 (1992) 1589-1615.
[15] B. Jacrot, Study of biological structures by neutron-scattering from solution, Rep. Prog. Phys., 39 (1976) 911-953.
[16] D. Chapman, Nuclear Magnetic Resonance Spectroscopic Studies of Biological Membranes, Annals of the New York Academy of Science, 195 (1972) 179-206.
[17] R. Bansil, J. Day, RAMAN-SPECTROSCOPY AS A PROBE OF LIPID FLUIDITY IN DEUTERATED LIPID BILAYERS, Bulletin of the American Physical Society, 23 (1978) 282-282.
[18] I.C.P. Smith, H.H. Mantsch, LOOK AT MEMBRANES BY FOURIER-TRANSFORM NMR AND IR OF DEUTERATED LIPIDS, Trends in Biochemical Sciences, 4 (1979) N152-N154.
[19] A.P. Tulloch, SYNTHESIS, ANALYSIS AND APPLICATION OF SPECIFICALLY DEUTERATED LIPIDS, Progress in Lipid Research, 22 (1983) 235-256.
[20] M.R. Morrow, J.P. Whitehead, D. Lu, Chain-length dependence of lipid bilayer properties near the liquid crystal to gel phase transition, Biophys. J., 63 (1992) 18-27.
[21] X.D. Peng, A. Jonas, J. Jonas, HIGH-PRESSURE H-2-NMR STUDY OF THE ORDER AND DYNAMICS OF SELECTIVELY DEUTERATED DIPALMITOYL PHOSPHATIDYLCHOLINE IN MULTILAMELLAR AQUEOUS DISPERSIONS, Biophysical Journal, 68 (1995) 1137-1144.
[22] D.D. Baldyga, R.A. Dluhy, On the use of deuterated phospholipids for infrared spectroscopic studies of monomolecular films: a thermodynamic analysis of single and binary component phospholipid monolayers, Chemistry and Physics of Lipids, 96 (1998) 81-97.
[23] T. Hauss, S. Dante, T.H. Haines, N.A. Dencher, Localization of coenzyme Q(10) in the center of a deuterated lipid membrane by neutron diffraction, Biochimica Et Biophysica Acta-Bioenergetics, 1710 (2005) 57-62.
[24] M.C. Biesinger, D.J. Miller, R.R. Harbottle, F. Possmayer, N.S. McIntyre, N.O. Petersen, Imaging lipid distributions in model monolayers by ToF-SIMS with selectively deuterated components and principal components analysis, Applied Surface Science, 252 (2006) 6957-6965.
[25] D. Kessner, M.A. Kiselev, T. Hauss, S. Dante, S. Wartewig, R.H.H. Neubert, Localisation of partially deuterated cholesterol in quaternary SC lipid model membranes: a neutron diffraction study, Eur. Biophys. J. Biophys. Lett., 37 (2008) 1051-1057.
[26] L. Xie, U. Ghosh, S.D. Schmick, D.P. Weliky, Residue-specific membrane location of peptides and proteins using specifically and extensively deuterated lipids and C-13-H-2 rotational-echo double-resonance solid-state NMR, Journal of Biomolecular Nmr, 55 (2013) 11-17.
[27] Y. Gerelli, A. de Ghellinck, J. Jouhet, V. Laux, M. Haertlein, G. Fragneto, Multi-lamellar organization of fully deuterated lipid extracts of yeast membranes, Acta Crystallographica Section D-Biological Crystallography, 70 (2014) 3167-3176.
[28] B. Skolova, K. Hudska, P. Pullmannova, A. Kovacik, K. Palat, J. Roh, J. Fleddermann, I. Estrela-Lopis, K. Vavrova, Different Phase Behavior and Packing of Ceramides with Long (C16) and Very Long (C24) Acyls in Model Membranes: Infrared Spectroscopy Using Deuterated Lipids, J. Phys. Chem. B, 118 (2014) 10460-10470.
[29] G. Jancso, W.A. Vanhook, CONDENSED PHASE ISOTOPE-EFFECTS (ESPECIALLY VAPOR-PRESSURE ISOTOPE-EFFECTS), Chemical Reviews, 74 (1974) 689-750.

[30] N.O. Petersen, P.A. Kroon, M. Kainosho, S.I. Chan, THERMAL PHASE-TRANSITIONS IN DEUTERATED LECITHIN BILAYERS, Chemistry and Physics of Lipids, 14 (1975) 343-349.
[31] J.H. Davis, DEUTERIUM MAGNETIC-RESONANCE STUDY OF THE GEL AND LIQUID-CRYSTALLINE PHASES OF DIPALMITOYL PHOSPHATIDYLCHOLINE, Biophysical Journal, 27 (1979) 339-358.
[32] J. Katsaras, R.F. Epand, R.M. Epand, Absence of chiral domains in mixtures of dipalmitoylphosphatidylcholine molecules of opposite chirality, Physical Review E, 55 (1997) 3751-3753.
[33] M.R. Vist, J.H. Davis, PHASE-EQUILIBRIA OF CHOLESTEROL DIPALMITOYLPHOSPHATIDYLCHOLINE MIXTURES - H-2 NUCLEAR MAGNETIC-RESONANCE AND DIFFERENTIAL SCANNING CALORIMETRY, Biochemistry, 29 (1990) 451-464.
[34] M.R. Morrow, J.H. Davis, CALORIMETRIC AND NUCLEAR-MAGNETIC-RESONANCE STUDY OF THE PHASE-BEHAVIOR OF DILAUROYLPHOSPHATIDYLCHOLINE WATER, Biochimica Et Biophysica Acta, 904 (1987) 61-70.
[35] H.I. Petrache, S.W. Dodd, M.F. Brown, Area per lipid and acyl length distributions in fluid phosphatidylcholines determined by H-2 NMR spectroscopy, Biophysical Journal, 79 (2000) 3172-3192.
[36] N. Kucerka, J.F. Nagle, J.N. Sachs, S.E. Feller, J. Pencer, A. Jackson, J. Katsaras, Lipid bilayer structure determined by the simultaneous analysis of neutron and x-ray scattering data, Biophys. J., 95 (2008) 2356-2367.
[37] S. Lin, R.I. Duclos Jr., A. Makriyannis, Syntheses of 1,2-di-O-palmitoyl-sn-glycero-3-phosphocholine (DPPC) and analogs with 13C- and 2H-labeled choline head groups, Chemistry and Physics of Lipids, 86 (1997) 171-181.
[38] T.A. Darwish, E. Luks, G. Moraes, N.R. Yepuri, P.J. Holden, M. James, Synthesis of deuterated [D_{32}]oleic acid and its phospholipid derivative [D_{64}]dioleoyl-*sn*-glycero-3-phosphocholine, Journal of Labelled Compounds and Radiopharmaceuticals, 56 (2013) 520-529.
[39] M.C. Wiener, S.H. White, Fluid Bilayer Structure Determination by the Combined Use of X-Ray and Neutron-Diffraction .2. Composition-Space Refinement Method, Biophysical Journal, 59 (1991) 174-185.
[40] M.C. Wiener, S.H. White, Fluid Bilayer Structure Determination by the Combined Use of X-Ray and Neutron-Diffraction .1. Fluid Bilayer Models and the Limits of Resolution, Biophysical Journal, 59 (1991) 162-173.
[41] T. Heimburg, A model for the lipid pretransition: Coupling of ripple formation with the chain-melting transition, Biophysical Journal, 78 (2000) 1154-1165.
[42] G.S. Smith, C.R. Safinya, D. Roux, N.A. Clark, X-RAY STUDY OF FREELY SUSPENDED FILMS OF A MULTILAMELLAR LIPID SYSTEM, Molecular Crystals and Liquid Crystals, 144 (1987) 235-255.
[43] B. Kent, T. Hunt, T.A. Darwish, T. Hauss, C.J. Garvey, G. Bryant, Localization of trehalose in partially hydrated DOPC bilayers: insights into cryoprotective mechanisms, Journal of the Royal Society Interface, 11 (2014).
[44] B. KENT, C. GARVEY, T. LENNE, L. PORCAR, V. GARAMUS, G. BRYANT, Measurement of glucose exclusion from the fully hydrated DOPE inverse hexagonal phase, Soft Matter, 6 (2010) 1197-1202.
[45] M.C. Wiener, S.H. White, Structure of a Fluid Dioleoylphosphatidylcholine Bilayer Determined by Joint Refinement of X-Ray and Neutron-Diffraction Data .3. Complete Structure, Biophysical Journal, 61 (1992) 434-447.
[46] M.C. Pedersen, S.L. Hansen, B. Markussen, L. Arleth, K. Mortensen, Quantification of the information in small-angle scattering data, J. Appl. Crystallogr., 47 (2014) 2000-2010.
[47] S. Qian, D. Rai, W.T. Heller, Alamethicin Disrupts the Cholesterol Distribution in Dimyristoyl Phosphatidylcholine-Cholesterol Lipid Bilayers, J. Phys. Chem. B, 118 (2014) 11200-11208.
[48] S. Maric, N. Skar-Gislinge, S. Midtgaard, M.B. Thygesen, J. Schiller, H. Frielinghaus, M. Moulin, M. Haertlein, V.T. Forsyth, T.G. Pomorski, L. Arleth, Stealth carriers for low-resolution structure determination of membrane proteins in solution, Acta Crystallographica Section D-Biological Crystallography, 70 (2014) 317-328.
[49] M. Jamshad, V. Grimard, I. Idini, T.J. Knowles, M.R. Dowle, N. Schofield, P. Sridhar, Y.P. Lin, R. Finka, M. Wheatley, O.R.T. Thomas, R.E. Palmer, M. Overduin, C. Govaerts, J.M. Ruysschaert, K.J. Edler, T.R. Dafforn, Structural analysis of a nanoparticle containing a lipid bilayer used for detergent-free extraction of membrane proteins, Nano Research, 8 (2015) 774-789.
[50] A. Bremer, B. Kent, T. Hauss, A. Thalhammer, N.R. Yepuri, T.A. Darwish, C.J. Garvey, G. Bryant, D.K. Hincha, Intrinsically Disordered Stress Protein COR15A Resides at the Membrane Surface during Dehydration, Biophysical Journal, 113 (2017) 572-579.

Electronic Supplementary Material

Effect of deuteration on the phase behaviour and structure of lamellar phases of phosphatidylcholines – deuterated lipids as proxies for the physical properties of native bilayers

Gary Bryant[a*], Matthew B. Taylor[a], Tamim A. Darwish[b], Anton M. Krause-Heuer[b], Ben Kent[c] and Christopher J. Garvey[d*]

[a] **Centre for Molecular and Nanoscale Physics, School of Science, RMIT University, Melbourne, Australia**
[b] **National Deuteration Facility, Australian Nuclear Science and Technology Organisation, Lucas Heights, Australia**
[c] **Institute for Soft and Functional Materials, Helmholtz-Zentrum Berlin, Berlin, Germany**
[d] **Neutron Scattering, Australian Nuclear Science and Technology Organisation, Lucas Heights, Australia**

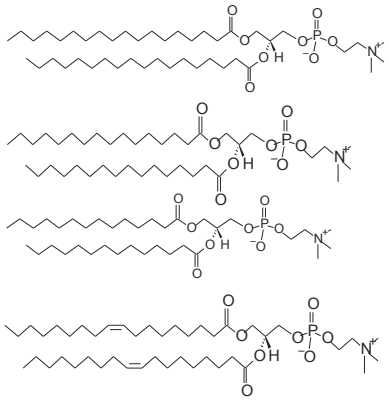

Figure S1: Lipids in this study, from top: DSPC, DPPC, DMPC, DOPC.

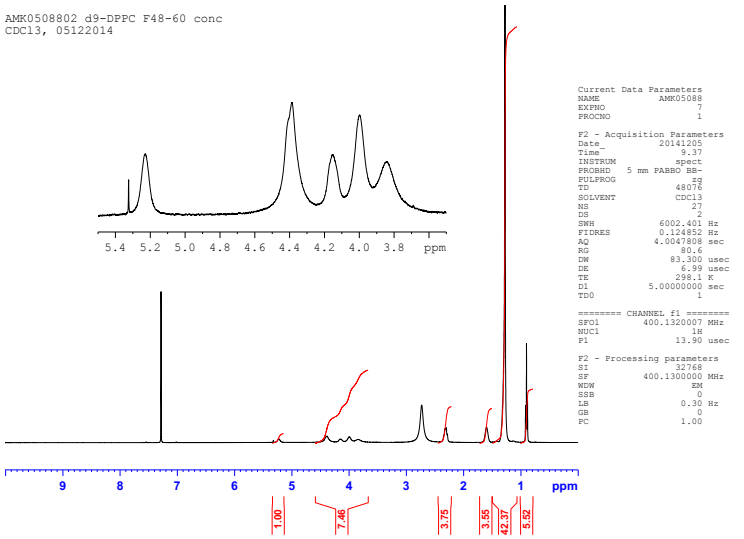

Figure S2. ^{1}H NMR (400 MHz, $CDCl_3$) of head-deuterated DPPC.

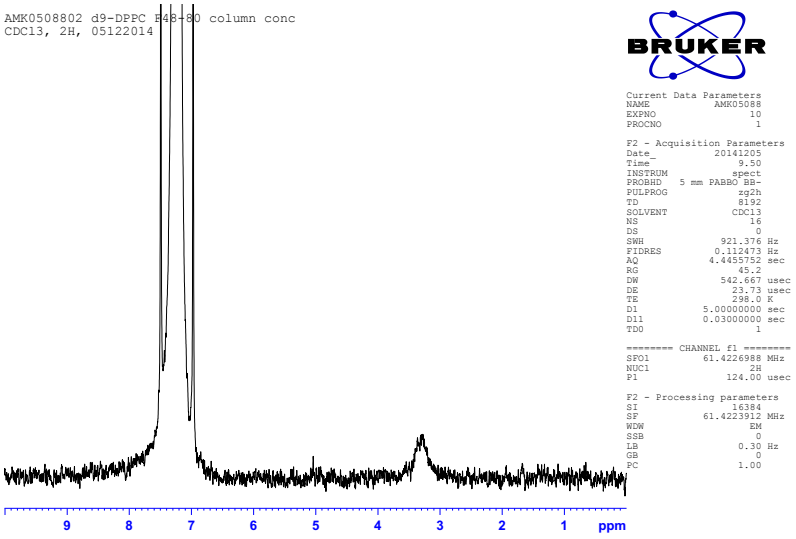

Figure S3. ^{2}H NMR ($CDCl_3$) of deuterated tail DPPC.

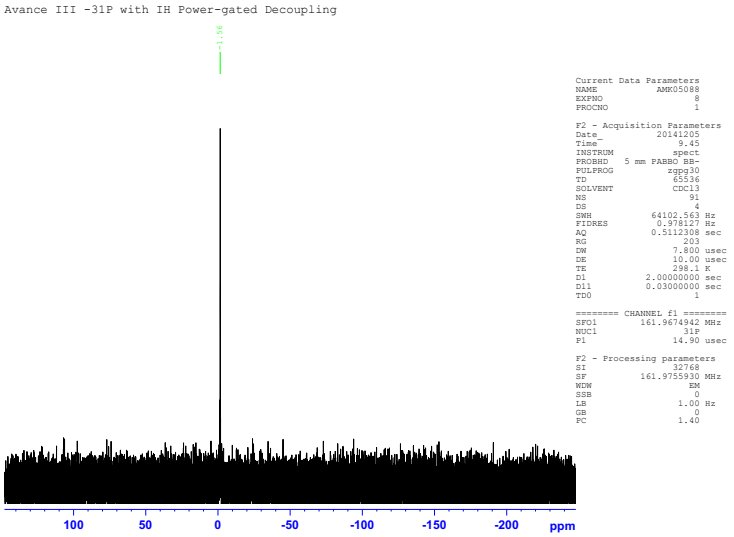

Figure S4. ^{31}P NMR ($CDCl_3$) of deuterated tail DPPC showing a single ^{31}P signal.

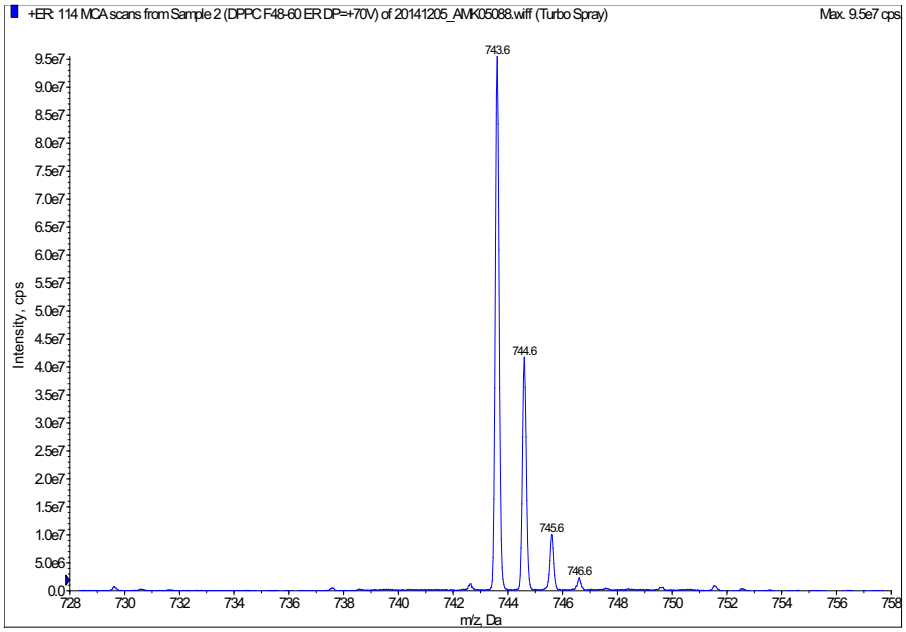

Figure S5. Enhanced resolution MS showing $[M+H]^+$ predicted 743.63, found 743.6.

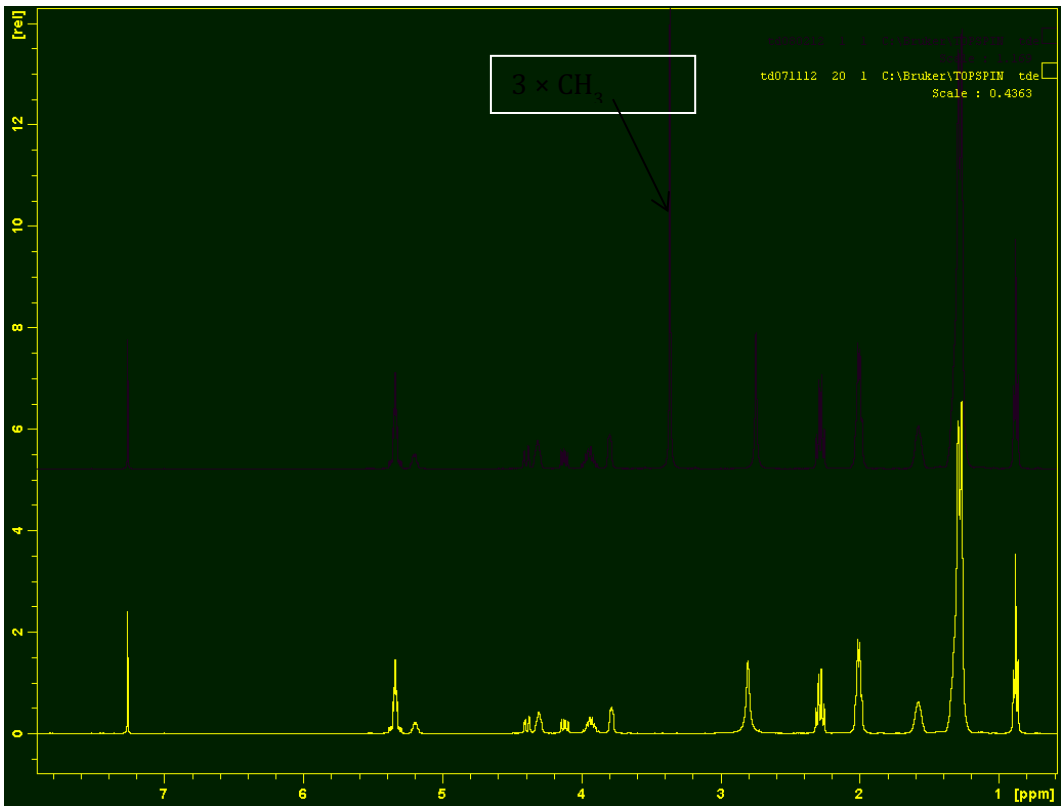

Figure S6. ^{1}H NMR (400 MHz, $CDCl_3$) of protiated (top) vs deuterated head DOPC (bottom).

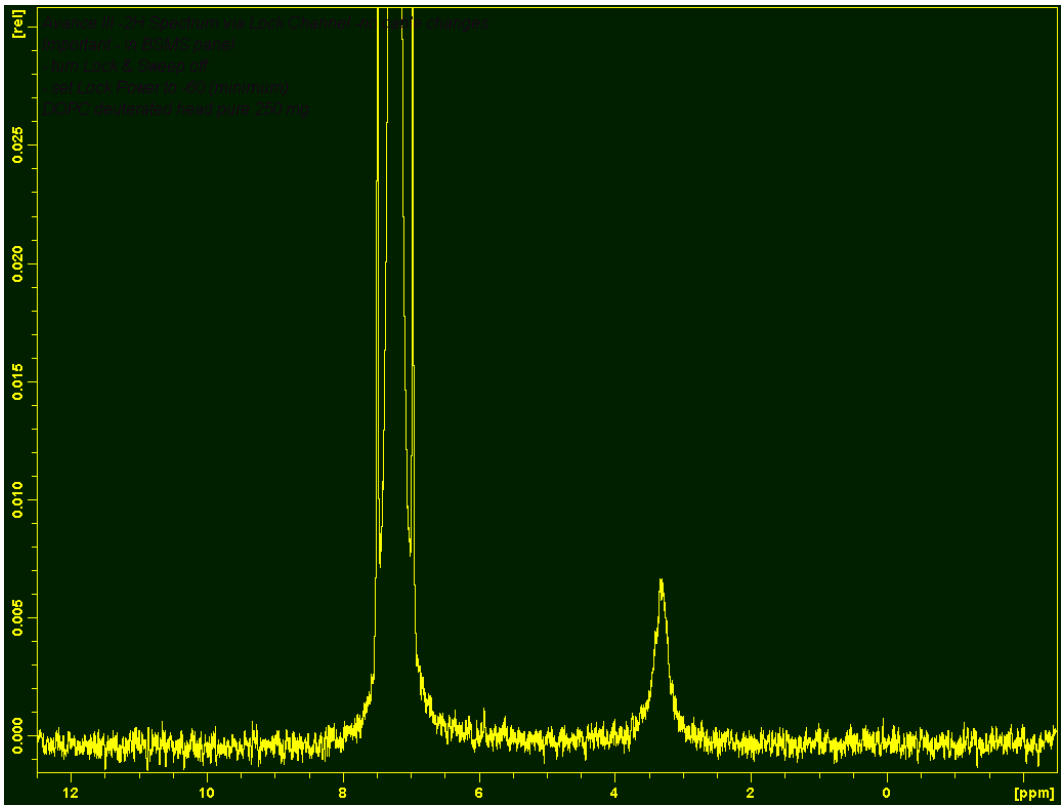

Figure S7. ^{2}H NMR ($CDCl_3$) of head deuterated DOPC.

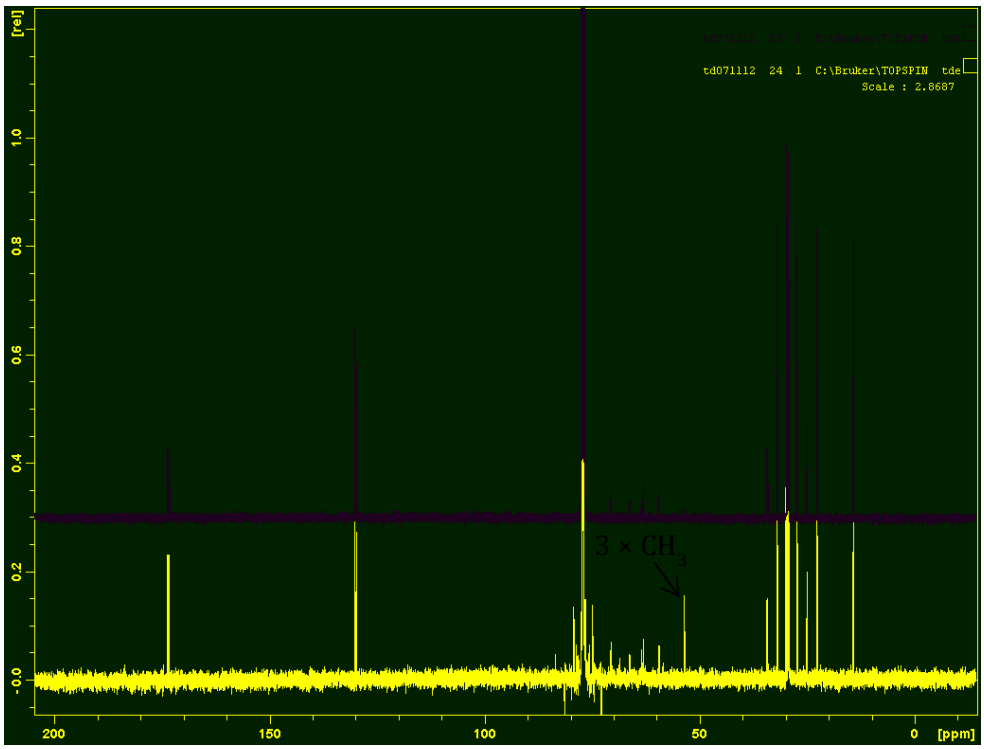

Figure S8. ^{13}C NMR (101 MHz, $CDCl_3$) of protiated (bottom) vs deuterated head DOPC (top).

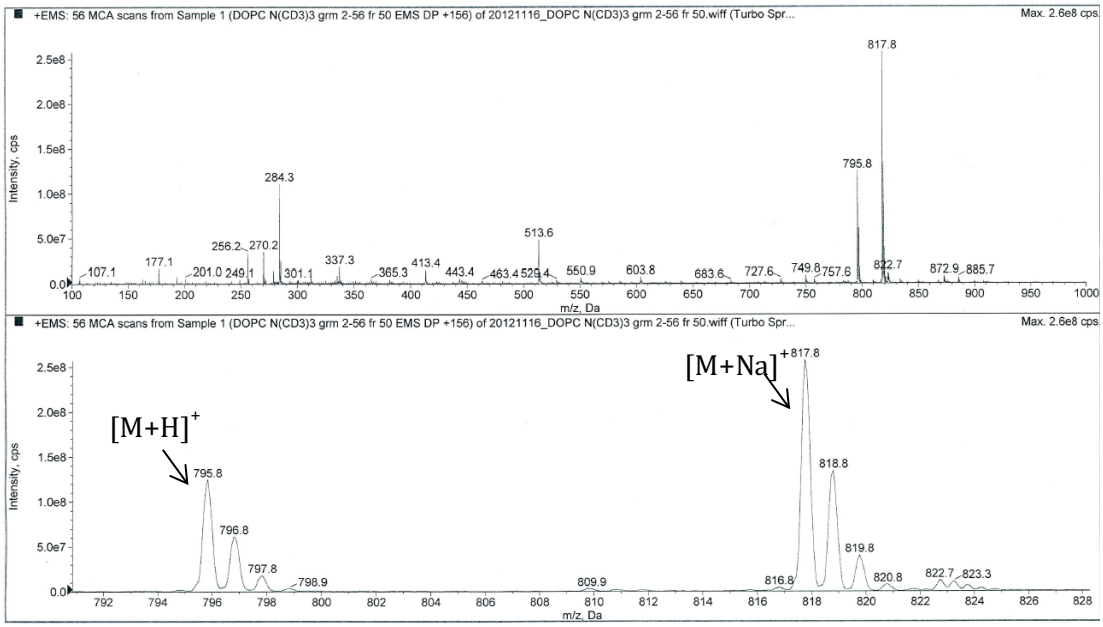

Figure S9. Mass spectrum (+ve mode) of head deuterated DOPC

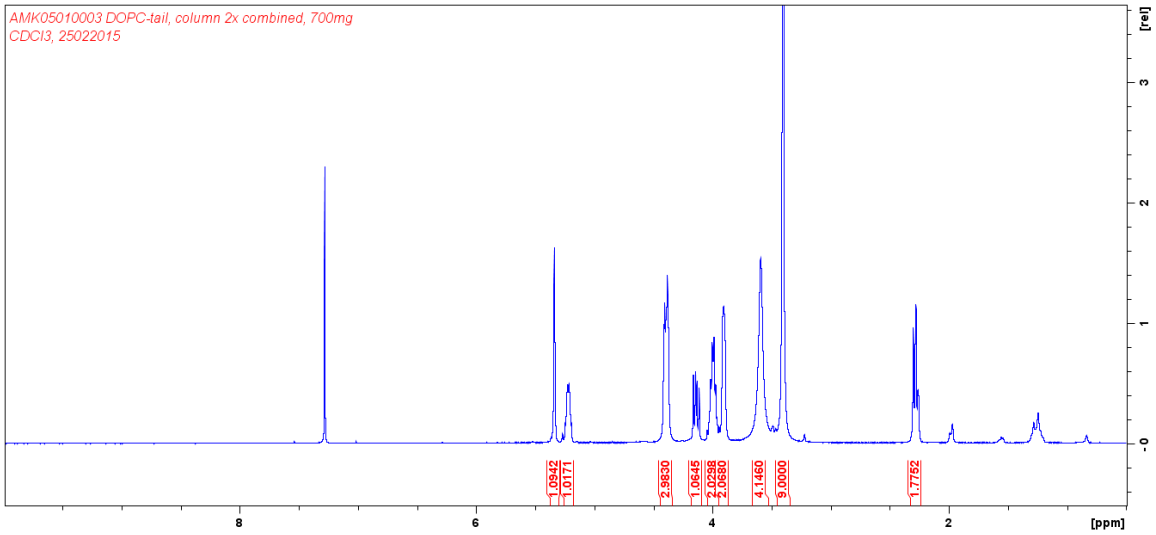

Figure S10. ^{1}H NMR ($CDCl_3$, 400 MHz) of deuterated tail DOPC.

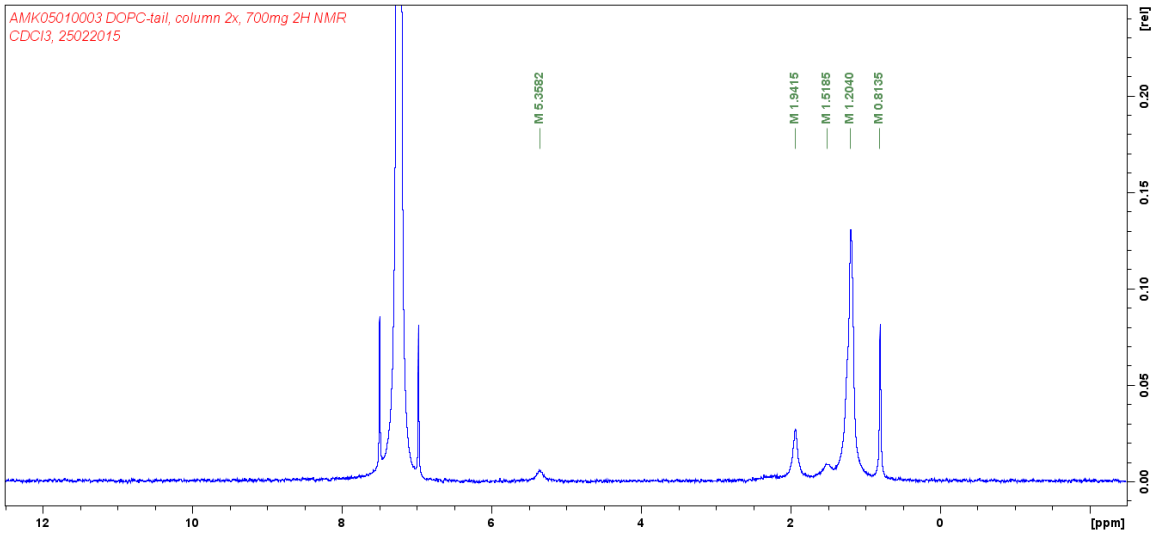

Figure S11. ^{2}H NMR ($CDCl_3$) of deuterated tail DOPC.

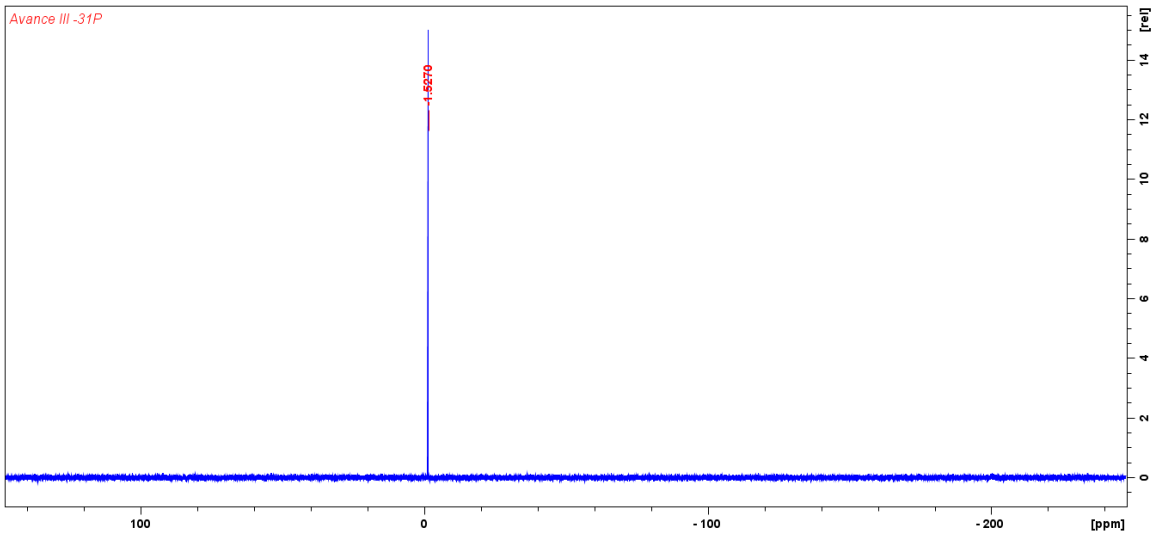

Figure S12. ^{31}P NMR ($CDCl_3$) of deuterated tail DOPC.

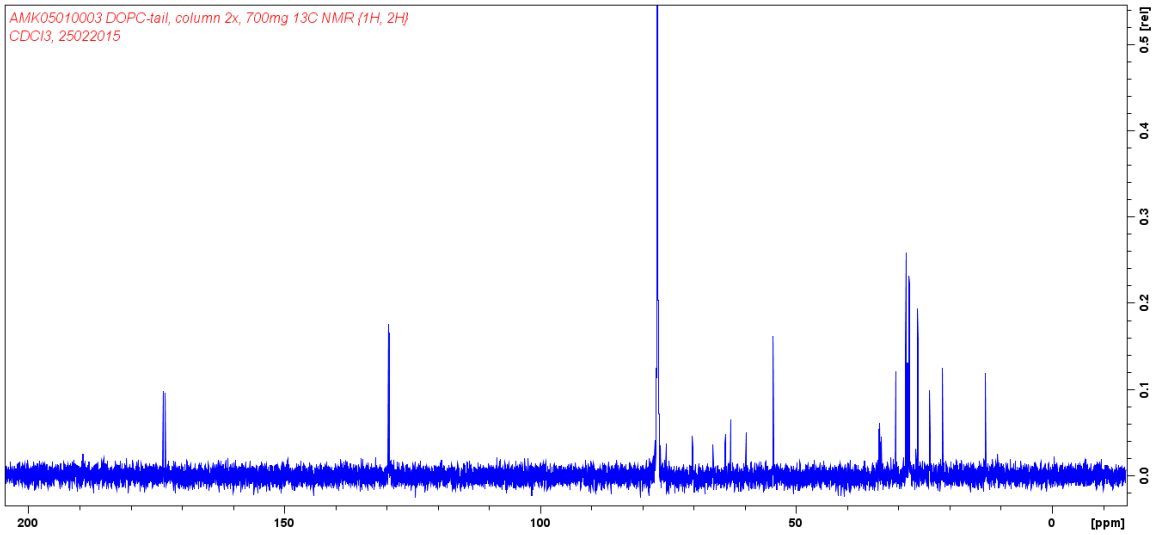

Figure S13. ^{13}C NMR ($CDCl_3$) {^{1}H, ^{2}H decoupled} of deuterated tail DOPC.

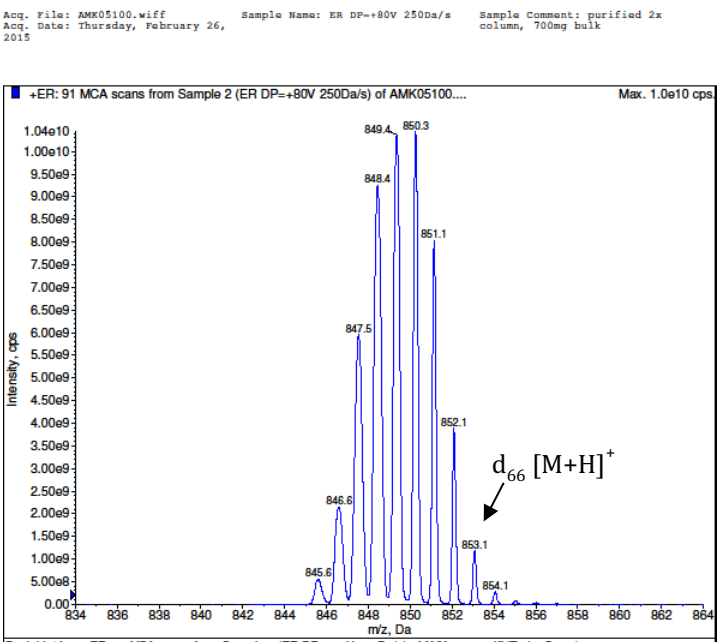

Peak List for " +ER: 91 MCA scans from Sample 2 (ER DP=+80V 250Da/s) of AMK05100.wiff (Turbo Spray)"

	m/z (Da)	Resolution	Intensity (cps)	Peak area (counts)	Charges	Width (Da)	% Intensity
1	845.6100	2284.3991	5.6312e8	7.4912e9	1	0.3702	5.3520
2	846.6000	2010.5050	2.1534e9	3.1400e10	Undefined	0.4211	20.8490
3	847.5300	2097.1642	5.9602e9	8.3625e10	1	0.4041	57.6190
4	848.4300	2105.7070	9.2573e9	1.2771e11	1	0.4029	88.9922
5	849.3600	2526.8705	1.0344e10	1.2016e11	1	0.3361	100.0000
6	850.2600	3437.2699	1.0436e10	9.0607e10	1	0.2474	99.7429
7	851.1300	4240.5259	8.0367e9	5.7746e10	1	0.2007	75.9034
8	852.0900	4790.9379	3.8917e9	2.4994e10	1	0.1779	36.4115
9	853.0800	4967.3589	1.1850e9	7.4128e9	1	0.1717	11.0622
10	854.0700	4942.7550	2.7849e8	1.7871e9	Undefined	0.1728	2.5927

Figure S14. Mass spectrum (+EMS) of deuterated tail DOPC.

Lipid	Chain length	MW	Measured temp – gel (°C)	Measured temp - fluid (°C)
DMPC	14	678	5	45
D-chain		732		
DPPC	16	734	20	75
D-chain		796		
DSPC	18	790	20	80
D-chain		861		
DOPC	18	786	--	10
D-chain		852		
D-head		794		

Table S1 Lipids used in this study, and the temperatures used for SAXS measurements.

			DOPC		D-Head		D-Tail	
Label	**Component**	**N**	**Formula**	**b**	**Formula**	**b**	**Formul**	**b**
1	Methyl	2	CH3	-0.914			CD3	4.920
2	Acyl inside	3.67	CH2	-0.305			CD2	6.831
3	Double bond	2	C2H2	1.162				
4	Acyl middle	7.18	CH2	-0.596			CD2	13.364
5	Acyl outside	17.15	CH2	-1.423			CD2	31.922
6	COO	2	CO2	3.650				
7	Glycerol	1	C5H5O4	0.124				
8	Phosphate	1	PO4	2.834				
9	Choline	1	C5H13N	-0.602	C5H4D9N	8.767		
10	Water	--	8% D2O	0				

Table S2. Molecular components used in the reconstruction, after the method of Wiener and White [1]. N is the number per lipid, b is the neutron scattering length in units of 10^{-12} cm. Head and tail deuterated DOPC share the same values as DOPC unless shown.

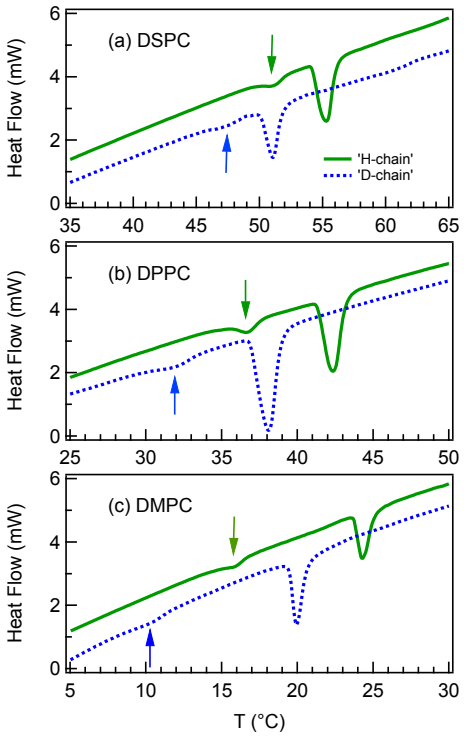

Figure S15 DSC scans during warming for the 3 saturated lipids and the chain-deuterated analogues: (a) DSPC; (b) DPPC; (c) DMPC; for protiated lipids (solid green lines) and chain-deuterated lipids (dotted blue lines). Arrows indicate the pre-transition. Scans are shifted vertically for clarity. The overall character of the scans is similar, with the chain-deuterated reflections shifted downwards by 4.3 ± 0.1°C.

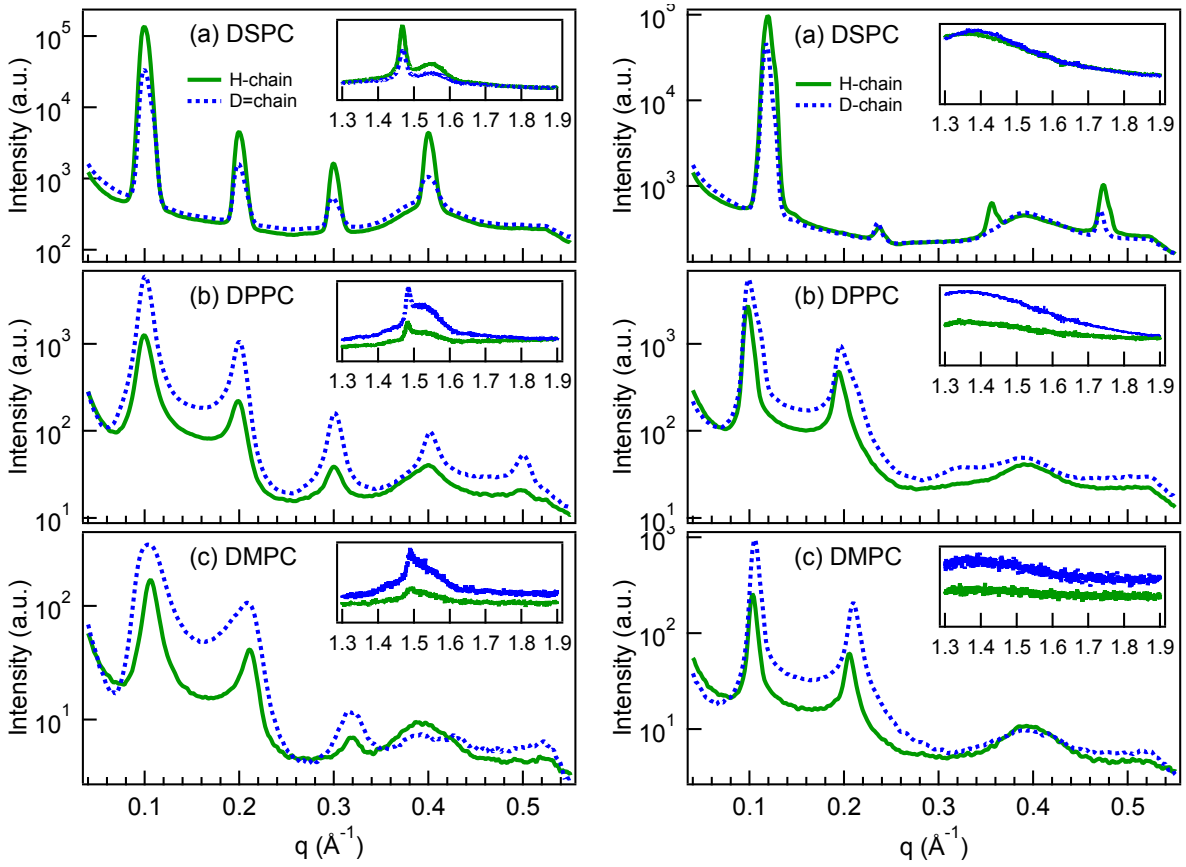

Figure S16 SAXS scattered intensities vs. scattering vector for (a) DSPC, (b) DPPC and (c) DMPC in the gel phase (left) and fluid phase (right) for protiated lipids (solid green lines) and chain-deuterated lipids (dotted blue lines). Insets show the wide angle (WAXS) data. The scan temperatures are given in Table S1. The broad reflection at 0.39Å is due to the Kapton windows on the DSC cell.

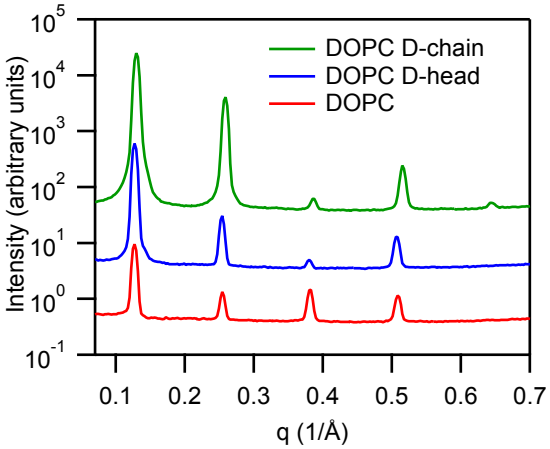

Figure S17 intensity vs. scattering vector curves determined from the theta - 2-theta scans of DOPC, D-chain and D-head, equilibrated at 75% relative humidity with an aqueous medium consisting of 8% D_2O and 92% H_2O. Scans are offset vertically for clarity.

Lipid	Repeat spacing (Å)	Std. Error (Å)
DOPC	49.39	0.01
D-chain	48.89	0.01
D-head	49.72	0.01

Table S3 Neutron membrane diffraction determination of repeat spacing for low hydration DOPC (75% RH, 8% D_2O).

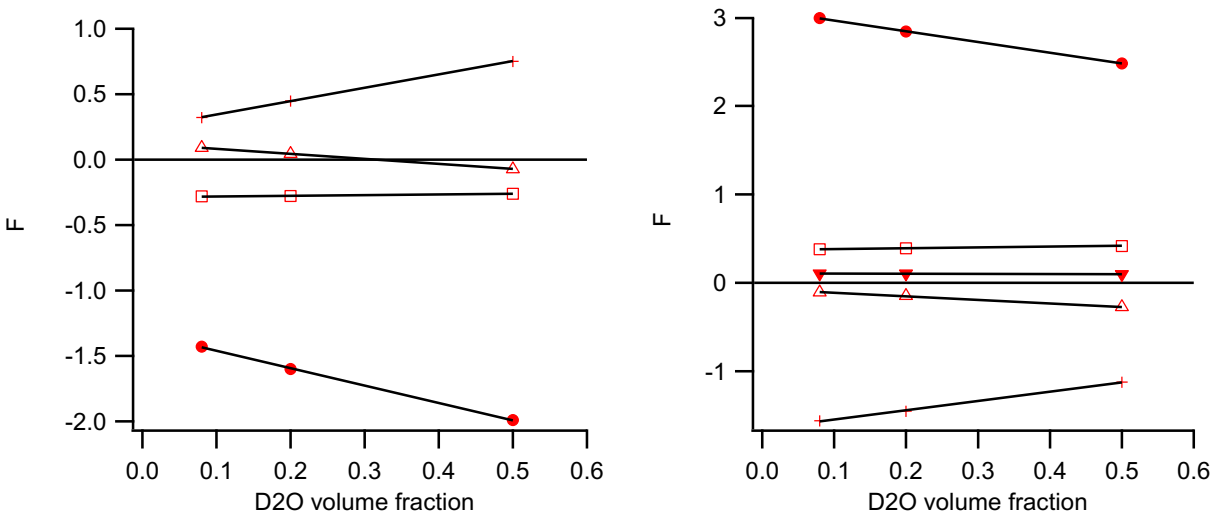

Figure S18. Phasing graphs of head deuterated DOPC (left) and chain deuterated DOPC (right).

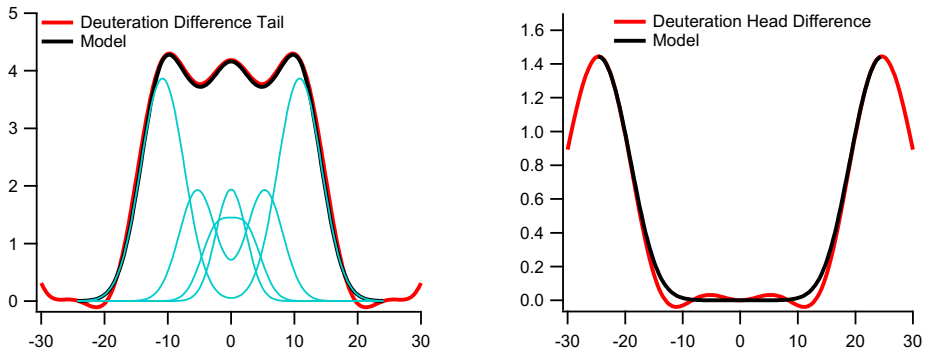

Figure S19. Left - the SLD difference between chain deuterated and protiated DOPC; Right - the SLD difference between head deuterated and protiated DOPC. The left hand figure shows the components in blue.

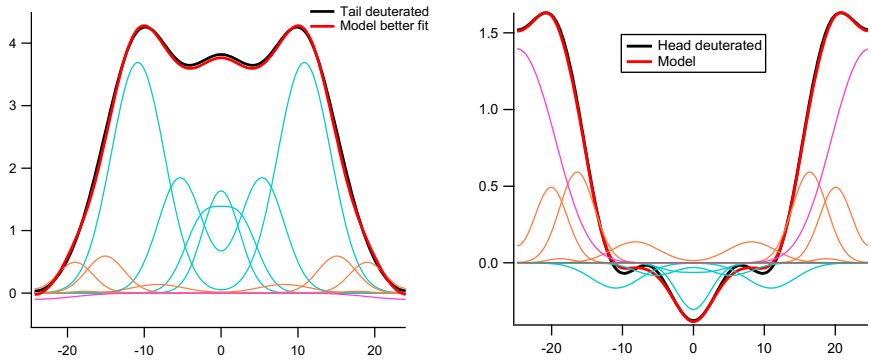

Figure S20. Chain deuterated DOPC (left) and head deuterated DOPC (right) SLD profiles and their quasi-molecular contributions, comparable to Figure 8 for DOPC.

References

[1] M.C. Wiener, S.H. White, STRUCTURE OF A FLUID DIOLEOYLPHOSPHATIDYLCHOLINE BILAYER DETERMINED BY JOINT REFINEMENT OF X-RAY AND NEUTRON-DIFFRACTION DATA .3. COMPLETE STRUCTURE, Biophys. J., 61 (1992) 434-447.